Journal of Materials and Electronic Devices 3 (2024) 21-29

JOURNAL OF MATERIALS AND ELECTRONIC DEVICES
JMED
http://dergi-fytronix.com/

Computational study of Be, Mg and Ca cations interacting with Isatin

Fatma KANDEMIRLI[1], Serap SENTURK DALGIC[2]

[1]Biomedical Engineering Department, Faculty of Engineering & Architecture, Kastamonu University, Kastamonu.
[2]Department of Physics, Faculty of Science, Trakya University, 22030 Edirne, Turkey
https://orcid.org/0000-0001-6097-2184
email: fkandemirli@yahoo.com

Theoretical investigation of isatin (Is) interaction with Be^{2+}, Mg^{2+}, and Ca^{2+} cations has been performed at the B3LYP/6-311G (d, p) level of Density Functional Theory (DFT). Be-Is_a, Mg-Is_a, Ca-Is_a, Be-Is_b, Mg-Is_b, Ca-Is_b complexes show -324.37, -192.55, -144.15, -230.482, -113.581, -72.23 kcal/mol interaction energy. Topology analyses such as the Quantum Theory of Atoms in Molecules (QTAIM) and the non-covalent index (NCI) analysis based on the reduced density gradient (RDG) method indicate that the interactions between the isatin and Be^{2+} cation are more substantial than those of the other cations. The non-covalent interactions between Is molecule and Be^{2+}, Mg^{2+}, and Ca^{2+} cations are evidenced by the colour-filled RDG isosurfaces. The aromaticity change of phenyl induced upon complex formation was evaluated with the Harmonic Aromaticity Oscillator Model (HOMA) index. The vertical electron affinity (VEA) and the vertical ionization energy (VIE) for Is molecule, Be^{2+}, Mg^{2+}, and Ca^{2+} cations and their complexes were calculated and Electron Donor-Acceptor Map (DAM) was drawn.

Keywords: Isatin, DFT, QTAIM, HOMA

Submission Date: 25 July 2024
Acceptance Date: 30 August 2024

**Corresponding author: serapd@trakya.edu.tr , dserap@yahoo.com*

1. Introduction

The two-dimensional (2D) 1H-indole-2,3-dione or 2,3-dioxindole called common name as isatin (Is) is an indole derivative. There are two cyclic rings, one of which is five-membered (antiaromatic character) and the other is six-membered (aromatic property) in its structure. A five-membered ring contains a nitrogen atom and also two carbonyl groups are bound to a member ring, and both rings lie in the same plane. It is found in plants of the genus Isatis, in Couroupita guianensis Aubl. [1] in Calanthe discolor LINDL.5 [2] and in humans, as it is a metabolic derivative of adrenaline [3-5]. Isatin is used as a nucleophile and an electrophile in synthetic chemistry. The most well-known reaction of Is as an electrophile is nucleophilic addition to the keto group in the third position. The aromatic ring and γ-lactam nitrogen behave as a nucleophile site.

They studied the optical anisotropic behaviour of Is in the solid state with density functional theory (DFT) calculations using both non-periodic and periodic approaches. Three polarization vector directions [100], [010], and [001] concerning the optical properties, the behaviours of the complex dielectric and conductivity functions as well as the refractive index and the extinction coefficient [6]. They

studied the ab initio theoretical and experimental data on the FTIR spectra of Is and six of its F, Cl, Br, I, NO_2, CH_3 derivatives to correlate these with the respective structural data and those of NacetylIs and reported that strong electron-donors shorten and stabilize the unusually long a-dicarbonyl CC bond. At the same time, electron-accepting groups tend to stretch this bond further. N-deprotonation causes the elongation of the five-membered ring along the NCCO vector and the widening of bonds within the α-dicarbonyl moiety [7].

Adsorption of organic molecules on metals is of great interest because it provides functionalization of surfaces. [8]. The bond between the surface and the adsorbate is an interaction between electrostatic interaction and covalent doping, including charge transfer (CT) to the surface [9].

Since the conductivity of a molecule is related to the potential energy of that molecule, as the potential energy decreases, its conductivity increases, and as the potential energy of the molecule increases, the stability of that molecule decreases [10].

According to Koopmans Theorem, it is seen that the ionization potential is the negative value of the E_{HOMO} of the molecular device in question [11].

By investigating the interaction of benzene and substituted benzene with alkali and alkali metal cations, fundamental aspects of the Cation-π interaction have been understood [12]. The interaction of isatin with Li^+, Na^+, K^+ ions in group IA was studied [13].

In this study interactions between Is and Be^{2+}, Mg^{2+}, and Ca^{2+} cations and the effects of metal complexation on the aromaticity of Is were studied and characteristics of critical Points (CPs) were calculated by Quantum theory of atoms in molecules (QTAIM) and Non-covalent index (NCI) analysis using the Multiwfn package and visual molecular dynamics (VMD) software [14, 15].

In order to understand the antioxidant capacity of Is when it interacts with Be, Mg and Ca cations and to investigate the effect of these cations on the properties of isatin, the interaction of isatin-metal complexes and the electron transfer process were investigated.

2. Materials and Method

Density functional theory (DFT) calculations of Is and Be^{2+}, Mg^{2+} and Ca^{2+} cation complexes were performed with the GAUSSIAN 09 software package [16]. Becke's three-parameter hybrid one [17] with the correlation functional of Lee, Yang and Parr, and 6-311G (d, p) basis set were used [18]. All the structures were fully optimized without symmetry restrictions. It was also performed with frequency analysis at the same B3LYP/6-311 G (d, p) level and real minima were obtained at non-imaginary frequencies.

Basis Set Superposition Errors (BSSE) using the Boys and Bernardi's counterpoise method are used to correct interaction energies [19]. The aromaticity of the Is ring and its complexes was calculated with the Harmonic Oscillator Model of Aromaticity (HOMA) at the B3LYP/6-311G (d, p) level of theory using Multiwfn-3. Single point energy calculations were performed for anionic and cationic states of optimized molecules to study the electron transfer process of positively charged molecules.

3. Results and Discussions

Theoretical studies with B3lyp functional and 6-311G(d,p) basis set have been conducted on Be^{2+}, Mg^{2+}, and Ca^{2+}metal ion –Is complexes for two types of interactions. In one of the interactions, the metal ions are placed near the oxygen atoms of the carbonyl group of isatin, and in the other, the metal ions are placed at the top of the phenyl group belonging to the Is group. The optimized form, HOMO–LUMO orbitals and ESP for Is and its complexes computed at B3LYP level with 6-311G(d,p) basis set and generated via Gauss view 5.0, are shown in **Fig.1**.

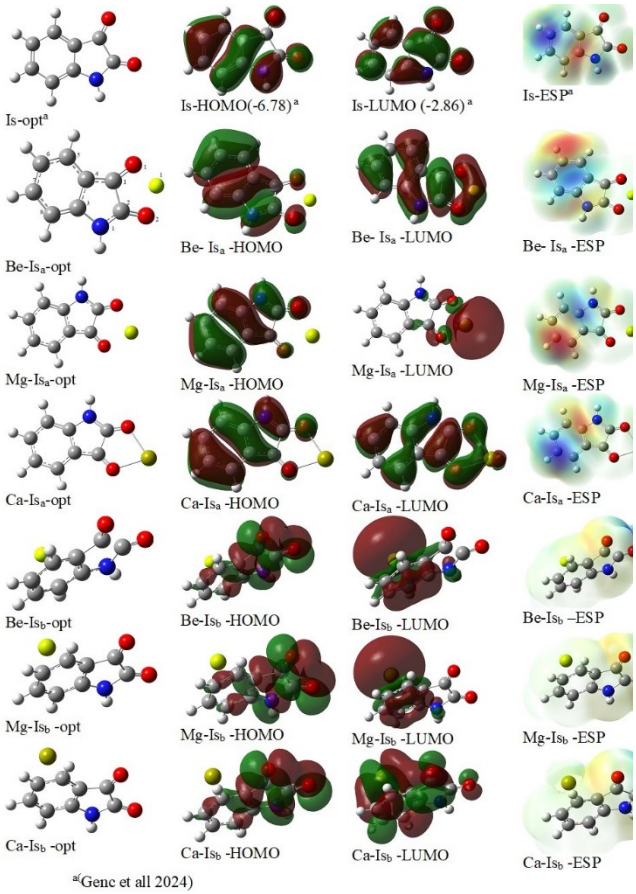

Fig.1. Optimized form, HOMO, LUMO and ESP shape of Is, Be-Is$_a$, Mg-Is$_a$, Ca-Is$_a$, Be-Is$_b$, Mg-Is$_b$, Ca-Is$_b$

Table 1 shows which atomic orbitals the HOMO and LUMO of Is, Be-Is_a, Mg-Is_a, Ca-Is_a, Be-Is_b, Mg-Is_b, Ca-Is_b complexes consist of and what their contributions are. The HOMO of the Is molecule consists of O10, O11, N1, C4, C8, C3, C2 C5, C9, C10, C11 atoms and their percentage contribution are 2.3, 7.8, 24.3, 12.1, 12.8, 0.33, 1.0, 10.3, 21.9, 3.8. The HOMO of the Be-Is_a consists of O10, O11, N1, C4, C8, C3, C2 C5, C9, C6, C11, C10, C11 atoms and their percentage contribution are 0.9, 2.7, 8.0, 5.0, 21.0, 1.0, 2.9, 13.8, 9.6, 28.8, 5.8, 0.2.

Table 1 Contribution of atoms orbitals to HOMO and LUMO for Is, Be-Is_a, Mg-Is_a, Ca-Is_a, Be-Is_b, Mg-Is_b, Ca-Is_b complexes

Atoms	Is	Be-Is_a	Be-Is_b	Mg-Is_a	Mg-Is_b	Ca Is_a	Ca Is_b
	HOMO						
O10	2.3	0.9	31.6	0.9	32.3	1.0	32.0
O11	7.8	2.7	34.3	3.4	34.0	3.7	34.3
N1	24.3	8.0	6.4	9.6	5.9	10.7	5.7
C4	12.1	5.0	8.6	5.6	8.3	6.1	8.1
C8	12.8	21.0	0.5	20.4	0.5	19.9	0.5
C3	0.3	1.0	7.5	1.0	7.9	1.0	8.1
C2	1.0	2.9	7.8	2.7	8.0	2.5	8.1
C5	2.7	13.8	0.4	12.7	0.5	11.7	0.5
C9	10.3	9.6	0.8	9.9	0.7	9.9	0.7
C6	21.9	28.8	0.5	28.2	0.5	27.8	0.4
C7	3.8	5.8	0.1	5.1	0.1	4.9	0.1
17 M		0.2	0.2	0.2	0.0	0.3	0.1
	LUMO						
O10	20.7	8.1	0.2	1.9	0.1	12.9	9.9
O11	9.9	4.6	0.1	1.8	0.2	7.1	3.1
N1	0.8	5.1	0.8	0.1	0.8	3.6	0.1
C4	5.6	1.5	0.0	0.1	0.4	0.7	12.6
C8	6.7	6.6	0.7	0.1	1.1	6.9	3.1
C3	22.1	23.0	0.1	0.6	-0.1	25.1	6.0
C2	10.9	14.6	0.0	0.6	0.0	14.4	2.0
C5	9.4	13.5	0.0	0.0	1.2	11.3	11.3
C9	0.9	3.0	0.5	0.0	0.9	1.3	7.5
C6	0.9	0.4	0.1	0.0	0.2	0.4	0.8
C11	12.0	15.6	0.3	0.0	1.2	12.7	15.0
17 M		3.8	97.7	94.8	94.3	3.4	28.1

As seen from the Table 1, the contribution of C8, C3, C2, C5, C6, C7 atoms to HOMO increases and those of O10, O11, N1, C4, C9 atoms to HOMO decreases at Be-Is_a, Mg-Is_a, Ca-Is_a, complexes. However, the contribution of O10, O11, C3, C7, atoms to HOMO increases and those of N1, C4, C8, C5, C9, C3, C2 atoms to HOMO decreases at Be-Is_b, Mg-Is_b, Ca-Is_b complexes. The LUMO of the Is molecule consists of O10, O11, N1, C4, C8, C3, C2 C5, C9, C10, C11 atoms and their percentage contribution are 2.33, 7.82, 24.3, 12.1, 12.8, 0.3, 1.0, 10.3, 21.9, 3.8. The HOMO of the Be-Is_a consists of O10, O11, C4, C8, C3, C7 C8, C11 atoms and their percentage contribution are 20.7, 9.9, 5.6, 6.7, 22.1, 10.9, 9.4, 12.0 [13]. The contribution of O10, O11 and C4 atoms to LUMO decreases for Be-Is_a, Mg-Is_a, Ca-Is_a, Be-Is_b, Mg-Is_b, Ca-Is_b complexes (Table 1).

As the ion size increases from Be^{2+} to Ca^{2+}, the distance of the metal ions from the oxygen atoms also increases. Likewise, the distance of the centre of the phenyl group of isatin from the metal ion also increases when going from Be^{2+} to Ca^{2+} (Table 2).

Table 2 The bond length between the interacting atoms for complexes

Structure	O10-M	O11-M	CT(Is_a-M)
Be-Is_a	1.53601	1.54554	1.247
Mg-Is_a	1.98188	1.98172	0.689
Ca-Is_a	2.24945	2.24945	0.424
Structure	Ph-M	**CT(Is_a-M)**	
Be-Is_b	1.28019	1.599	
Mg-Is_b	1.94056	0.943	
Ca-Is_b	2.37323	0.486	

The amount of charge transfer (CT) from Is to Be^{2+}, Mg^{2+} and Ca^{2+} cation^{2+} is 1.247, 0.689 and 0.424 for Be-Is_a, Mg-Is_a, Ca-Is_a complexes and 1.599, 0.943 and 0.486 for Be-Is_b, Mg-Is_b, Ca-Is_b complexes. The amount of charge transfer can be used as an indicator of the adsorption strength between Is and cations for both complexations. The largest CT is seen for Be-Is_b (Table 2).

Adsorption, interaction and deformation energies of metal complexes of isatin in terms of electronic energy, enthalpy and Gibbs free energy are summarized in Table 3. As predicted, the adsorption energy, enthalpy and Gibbs free energy of Be^{2+}, $Mg^{2+}$and Ca^{2+} complexes decrease with the increase of ion size (Be^{2+}, $Mg^{2+}$and Ca^{2+}).

All the complexes are stable and true minima in the potential energy surface, and interaction energy for Be-Is_a, Mg-Is_a, Ca-Is_a, Be-Is_b, Mg-Is_b, Ca-Is_b complexes are -324.37, -192.55, -144.15, -230.48, -113.58, -72.23 kcal/mol, respectively. Electronic energy, enthalpy and Gibbs free energy are summarized for studied complexes in Table 3. Interaction energy values decrease with the increasing cation equilibrium distance from the oxygen atoms of carbonyl group or geometric centre of the phenyl ring [20].

The adsorption energy values have the following order: Be-Is_a > Mg-Is_a > Ca-Is_a for the interaction oxygen atoms of

isatin with Be^{2+}, $Mg^{2+}$and Ca^{2+} ions, and Be-Is_b > Mg-Is_b > Ca-Is_b for the interaction phenyl group of Is with Be^{2+}, Mg^{2+} and Ca^{2+} ions. (Table 3). As seen the adsorption energy values are found to be strongly dependent on the size of the cation at both of calculation [12, 13].

Table 3 Adsorption, Interaction and Deformation energies for Be-Is_a, Mg-Is_a, Ca-Is_a, Be-Is_b, Mg-Is_b, Ca-Is_b complexes

		ΔE	ΔH	ΔG
Be-Is_a	E_{ads}	-295.81	-297.22	-287.60
	E_{int}	-324.37	-325.49	-316.48
	E_{def}	28.56	28.27	28.88
Mg-Is_a	E_{ads}	-179.43	-180.36	-171.08
	E_{int}	-192.55	-193.24	-184.51
	E_{def}	13.12	12.88	13.42
Ca-Is_a	E_{ads}	-132.87	-133.55	-124.68
	E_{int}	-144.15	-144.60	-136.26
	E_{def}	11.28	11.06	11.58
Be-Is_b	E_{ads}	-219.61	-220.62	-211.79
	E_{int}	-230.48	-231.63	-222.36
	E_{def}	10.87	11.01	10.58
Mg-Is_b	E_{ads}	-107.07	-107.56	-99.21
	E_{int}	-113.58	-114.15	-105.57
	E_{def}	6.51	6.59	6.36
Ca-Is_b	E_{ads}	-68.07	-68.41	-60.35
	E_{int}	-72.23	-72.64	-64.37
	E_{def}	4.16	4.22	4.02

HOMO–LUMO energy gap ΔE, which is the difference between the highest occupied molecular orbital energy (E_{HOMO}) and the lowest unoccupied molecular orbital energies (E_{LUMO}), of the Is and its complexes with the Be^{2+}, Mg^{2+} and Ca^{2+} ions, ΔE, E_{HOMO}, E_{LUMO}, computed at B3LYP level with 6-311G(d, p) basis set are shown in Fig.2.

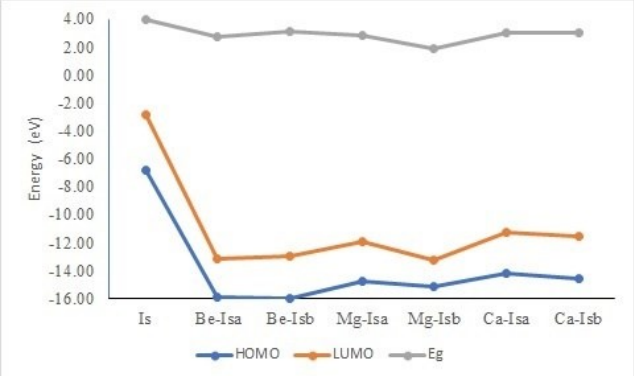

Fig.2. HOMO LUMO and Band gap energies of Is, Be-Is_a, Mg-Is_a, Ca-Is_a, Be-Is_b, Mg-Is_b, Ca-Is_b complexes

The negative value of E_{HOMO}, and E_{LUMO} decrease noticeably when the Is was adsorbed to the Be^{2+}, Mg^{2+} and Ca^{2+} ions. E_{HOMO} of Is is -6.78 eV while that of Be-Is_a, Be-Is_b, Mg-Is_a, Mg-Is_b, Ca-Is_a, and Ca-Is_b complexes are -15.90, -15.99, -14.77, -15.10, -14.20, -14.56 eV. The greatest energy reduction in E_{HOMO} was observed in the Mg-Is_b complex. The LUMO energy of Is is -2.86 eV and the greatest energy reduction for E_{LUMO} was observed also in the Mg-Is_b complex. The energy gap of Is is 3.92 eV, those of Be-Is_a, Be-Is_b, Mg-Is_a, Mg-Is_b, Ca-Is_a, and Ca-Is_b complexes are 2.72, 3.06, 2.80, 1.85, 2.98, 3.03 eV indicate that the HOMO-LUMO energy gap is greater if the metal ion interacts with the phenyl group of isatin (**Fig. 2**). In general, the lower the energy gap means the better the electron transfer process can be.

Quantum Theory of Atoms in Molecules (QTAIM) analysis

To obtain more information about the binding of Is with M (Be^{2+}, Mg^{2+} and Ca^{2+} ions), the topological parameters such as electron density ($\rho(\boldsymbol{r})$) and Laplacian ($\nabla^2\rho(\mathbf{r})$), total electron energy density ($V(\boldsymbol{r})$), potential electron energy density ($V(\boldsymbol{r})$) ve Lagrange kinetic energy ($G(\mathbf{r})$) at the bond critical point (BCP) involved in intermolecular hydrogen bonds were calculated using Bader's Theory of Atoms in Molecules (AIM) as known QTAIM [21](Table4).

Table 4. The QTAIM topological parameters of the Is-adsorbed compounds

Structure	BCPs Drug/NT	ρ_{BCP}	G_{BCP}	V_{BCP}
Be-Is_a	O10-Be	0.103229	0.185876	-0.199219
	O11-Be	0.099747	0.178137	-0.189793
Be-Is_b	Ph-Be	0.063640	0.072543	-0.092787
Mg-Is_a	O10-Mg	0.489624	0.077694	-0.066528
	O11-Mg	0.048638	0.077494	-0.066155
Mg-Is_b	Ph-Mg	0.029429	0.031468	-0.029999
Ca-Is_a	O10-Ca	0.049936	0.581967	-0.053534
	O11-Ca	0.050364	0.059467	-0.054635
Ca-Is_b	Ph-Ca	0.027407	0.021200	-0.020888
		H_{BCP}	$\nabla^2\rho_{BCP}$	$\lvert V_{BCP}\rvert/G_{BC}$
Be-Is_a	O10-Be	-0.013344	0.690128	1.071789
	O11-Be	-0.011657	0.665920	1.065436
Be-Is_b	Ph-Be	-0.020244	0.209193	1.279070
Mg-Is_a	O10-Mg	0.011166	0.355440	0.856279
	O11-Mg	0.011338	0.355330	0.853686
Mg-Is_b	Ph-Mg	0.001468	0.131745	0.953336
Ca-Is_a	O10-Ca	0.004663	0.251438	0.091988
	O11-Ca	0.004832	0.257196	0.918750
Ca-Is_b	Ph-Ca	0.000312	0.086049	0.985287

The observed molecular topological map of C=O groups and phenyl group of Is with Be^{2+}, Mg^{2+} and Ca^{2+} ions are given in Fig. 3.

With the help of QTAIM [21] it is now possible to describe the structure of molecules quantum mechanically. This theory has been widely applied to unravel atom-atom interactions in molecules, molecular clusters, small molecular crystals, proteins, covalent and non-covalent interactions in DNA base pairing and stacking [22,23]. It has been also considered to study the type of interactions between the molecules and nanomaterials such as carbon and silicon based nanotubes [24-26] and nanoribbons [27].

Defining the concept of bonding via bond pathways and bond critical points (BCPs) has been found to be extremely useful in interpreting the topological properties of electron density (ED) and its derivatives. In general if $\rho(\mathbf{r})$> 0.20 au in shared (covalent) bonding and if $\rho(\mathbf{r})$< 0.10 au in a closed-shell interaction [28]. Generally speaking, the larger the electron density value in BCP, the stronger the bond.

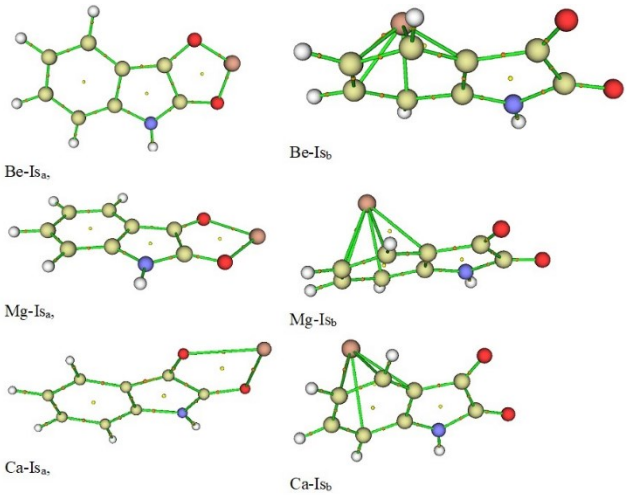

Fig.3. The QTAIM molecular graphs between attractive atom pairs at BCPs.

From Table 4, for the Be-Is_a, Mg-Is_a, Ca-Is_a complexes, the values of ρ_{BCP} for O10-Be, O11-Mg, O10-Ca bond lengths are 0.103229, 0.489624, 0.049936, and those for O11-Be, O11-Mg, O11-Ca bond lengths are 0.099747, 0.048638, 0.503641. The strongest bond is calculated for Be-IS_a complex. Laplacian of $\rho(\boldsymbol{r})$ is expressed as following by viral theorem

$$\frac{1}{2}\nabla^2\rho(\mathbf{r}) = 2G(\mathbf{r}) + V(\boldsymbol{r}) \qquad (1)$$

Where, $2G(\mathbf{r})$, $V(\boldsymbol{r})$, and $\nabla^2\rho(\mathbf{r})$ represent the electronic kinetic energy density, the electronic potential energy density and the excess potential energy at BCP. A positive $\nabla^2\rho(\mathbf{r})$ at a BCP means that the contribution of kinetic energy is bigger than that of potential energy and indicates depletion of electronic charge along the bond path.

If $\nabla^2\rho(\mathbf{r})$ is negative charge concentration occurs. In covalent bonding the two negative curvatures are dominant and $\nabla^2\rho(\mathbf{r})$ is negative. In contrast, ionic, hydrogen-bonding or van der Walls interactions are characterized by a depletion of density in the region of contact of the two atoms [28].

$\nabla^2\rho(\mathbf{r})$ is positive for C=O10 group and C=O11 group of Is belonging Be-Is_a, Mg-Is_a, Ca-Is_a complexes and the distance between phenyl group of Is and M ion belonging Be-IS_b, Mg-Is_b, and Ca-Is_b complexes. Considering that kinetic and potential energy densities have equal weights, Cremer and Kraka proposed to evaluate the total electronic energy density in BCP with the following formula [29].

$$H(\mathbf{r}) = G(\mathbf{r}) + V(\boldsymbol{r}) \qquad \textbf{(2)}$$

Table 4 obtains a positive value $\nabla^2\rho_{BCP}$ and negative value H(r) for ionic and coordinate bonds. Based on the ratio $|V_{BCP}|/G_{BCP}$, for the closed shell interaction $V_{BCP}|/G_{BCP}$ <1 and for the shared shell interaction $|V_{BCP}|/G_{BCP}$ >2. The interaction for the intermediate type refers to the ratio falls between these two limits. Some strong bounds have a |V|/G ratio value greater than 1.0 and it is taken into account for partially covalent interactions. As seen in Table 4, the interactions in Be-Is_a and Be-Is_b complexes show partially covalent character because of the values of $|V_{BCP}|/G_{BCP}$ >1. The other |V|/G ratio values are $|V_{BCP}|/G_{BCP}$ <1, thus, those interactions refer to non-covalent bonds. On this line, the non-covalent index (NCI) analysis was performed using the reduced density gradient (RDG) method.

The Non-Covalent Index (NCI) –Reduced Density Gradient (RDG) Analysis

To identify the interaction as a non-covalent bond character clearly, the NCI theory [30, 31]. gives qualitative information using a colour scale (as given in Figure 4), i.e. blue, green and red. These colours indicate strong, attractive, weak, and strong repulsive interactions. The NCI analysis based on the RDG method can be considered an extension of the QTAIM theory for visual study. The RDG function, which is the derivative of electron density [32, 33] has been computed using the Multiwfn package to determine the non-covalent interactions through the sign (λ2), which is the largest Hessian matrix of ρ(r). The NCI plots are illustrated in Figure 4 (left side) for Be-Isa and Mg-Isa structures at 0.5 isosurface value by plotting RDG versus sign (λ2) ρ using the Multiwfn program package [14]. The value of sign (λ2) ρ in Fig. 4 is represented by filling colour according to the colour bar at the top of Fig. 4. according to the colour bar as given at the top of the Fig. 4.

In Fig. 4, red regions refer to steric interactions, blue regions to the strong, attractive interactions and green areas to van der Waals interactions. The typical non-covalent and covalent bonds can be distinguished from the NCI plots. In the non-covalent bonds, a green mixed with blue colour isosurface refers to a moderate attractive interaction observed in the NCI plots. The RDG isosurfaces between Isatin and Be^{2+} /Mg^{2+} obtained from VMD are also shown in Fig. 4 on the-hand side.

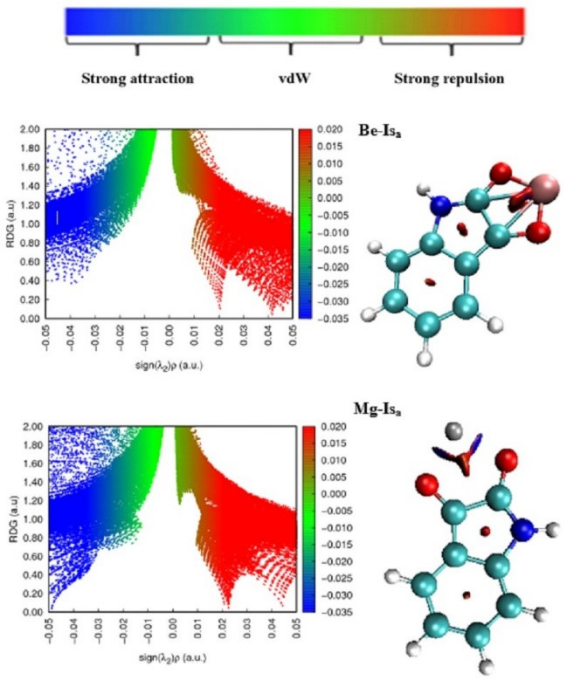

Fig.4 The NCI/RDG scatter plots (left) and the colour filled RDG isosurfaces (right) for (**a**) Be-Is_a and (**b**) Mg-Is_a structures where C, H, O, N, Be and Mg atoms are shown in cyan, white, red, blue, purple and silver, respectively.

Here, the three distinct spikes in the red region, precisely according to the value of sign (λ2) ρ(r) ranging from 0.02 to 0.045 a.u, describe the stabilizing steric interactions. These interactions are clearly visible due to the red–filled circles at the centre of both phenyl rings and over the bond between O-Be-O in the colour RDG isosurface for Be-Is_a. On the right-hand side of Fig. 4 (lower case), the blue-filled circles over the bonds between the Mg^{2+} cation and oxygen atoms of the Is molecule indicate the existence of attractive interactions. The red circles are observed at the centre of both phenyl rings of the Is molecule during the interaction with the Mg^{2+} cation.

HOMO aromaticity Index analysis

HOMA index was able to describe the geometry-based aromaticity of the studied compounds and are given in Table 5. HOMA index was defined by Kruszewski and Krygowski [34-36] and known as displacement in cyclic structures.

Table 5 HOMA and Bird aromaticity index value

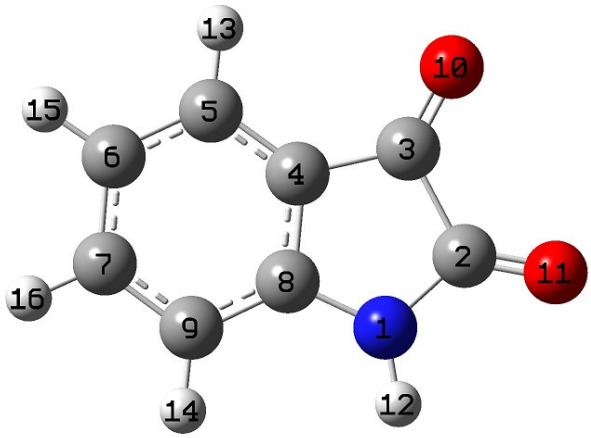

	Is	Be-Is_a	Be-Is_b	
Bonds	Atom pair Contribution for HOMA			
C5-C4	-0.000049	-0.052460	-0.012714	
C4-C8	-0.015338	-0.121813	-0.145283	
C8-C9	-0.000063	-0.040796	-0.098060	
C9-C7	-0.005141	-0.083103	-0.049283	
C7-C6	-0.003953	-0.005837	-0.057651	
C6-C5	-0.001640	-0.000130	-0.063048	
HOMA	0.973816	0.695862	0.573961	
Bonds	Mg- Is_a	Mg- Is_b	Ca-Is_a	Ca-Is_b
	Atom pair Contribution for HOMA			
C5-C4	-0.027720	-0.011966	-0.020470	-0.002446
C4-C8	-0.070341	-0.112131	-0.062750	-0.076327
C8-C9	-0.025038	-0.061823	-0.019995	-0.034075
C9-C7	-0.045796	-0.038168	-0.034632	-0.013956
C7-C6	-0.005820	-0.042693	-0.005631	-0.028272
C6-C5	-0.000006	-0.041071	-0.000001	-0.022882
HOMA	0.825279	0.692148	0.856521	0.822041
	Is	Be-Is_a	Be-Is_b	
Bonds	Atom pair Contribution for Bird aromaticity index			
C5-C4	1.814235	1.648384	1.733734	
C4-C8	1.725453	1.563610	1.541443	
C8-C9	1.825814	1.981763	1.588617	
C9-C7	1.764645	1.606123	1.653463	
C7-C6	1.771346	1.761084	1.640428	
C6-C5	1.788416	1.828486	1.632557	
BIRD	94.388074	75.020813	89.088597	
	Mg- Isa	Mg- Is_b	Ca Is_a	Ca Is_b
Bonds	Atom pair Contribution for Bird aromaticity index			
C5-C4	1.693893	1.736254	1.711170	1.781562
C4-C8	1.622477	1.573445	1.632981	1.614622
C8-C9	1.945713	1.634310	1.931986	1.680629
C9-C7	1.659244	1.672771	1.679530	1.729712
C7-C6	1.761167	1.664589	1.762117	1.692680
C6-C5	1.821520	1.667466	1.818903	1.705109
BIRD	81.25937	91.167408	83.14288	91.06353

Since C4-C8 deviates to ideal bond length for both Is and its complexes, it gives negative contribution to HOMA, that is this bond significantly braked aromaticity of Is especially in the complexes formed by Is with metal ions. The negative contribution order of C4-C8 to HOMA in studied complexes is Be-Is_b >Be-Is_a> Mg- Is_b> Ca-Is_b> Mg- Is_a> Ca-Is_a.
According to Table 5, it is obviously that BIRD index order is Mg-Is_b> Ca Is_b> Be-Is_b > Ca-Is_a > Mg- Is_a> Be-Is_a HOMA value of Is is 0.973816 near 1, however Be-Is_a, Mg-Is_a, Ca-Is_a, Be-Is_b, Mg-Is_b, Ca-Is_b are 0.695862, 0.825279, 0.856521, 0.573961, 0.692148, and 0.822041 denotes aroma city is affected by the interaction of Is and metal ion. Another geometry-based quantity is bird index [37]. The closer the bird index is to 100, the stronger the aromaticity.

Toxicity

The oxidative stress of all systems can be determined by calculating the electro-donating and electro-accepting forces. Good electron donors will donate their electrons. Good electron acceptors will accept electrons from other systems. The tendency to donate electrons (ω-) and the tendency to accept electrons(ω-) can be determined as following [34].

$$\omega^{+} = \frac{(VIP+3\,VEA)^2}{16(VIP-VEA)} \quad (3)$$

$$\omega^{-} = \frac{(3VIP+\,VEA)^2}{16(VIP-VEA)} \quad (4)$$

Where VEA and VIP denote vertical electron affinity and vertical ionization potential energy, respectively, calculated as follows:

$$A^{-1} \rightarrow A + 1e,\ VEA = \mathrm{E(A)} - E(A^{-1}). \quad (5)$$

$$\mathrm{A} \rightarrow A^{+1} + 1e,\ VIP = E(A^{+1})\text{-E(A)}, \quad (6)$$

Using the ω- and the ω+ values, DAM can be determined and is given in Fig. 5.

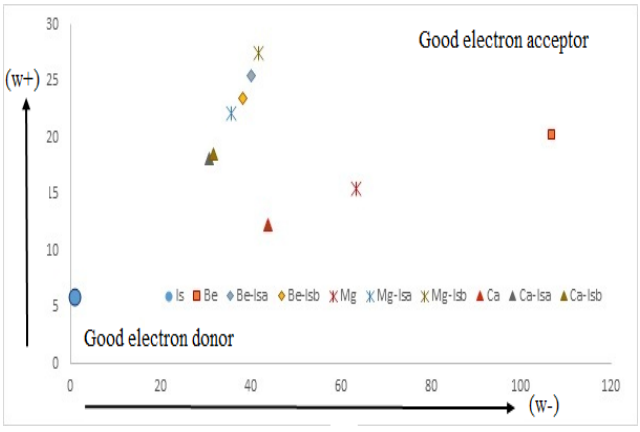

Fig.5 The DAM for Is, Be, Mg, Ca cations, Be-Is_a, Mg-Is_a, Ca-Is_a, Be-Is_b, Mg-Is_b, Ca-Is_b complexes.

If the systems below on the left are good electron donors, they donate electrons by producing reductions of other molecules that gain these electrons. The systems above on the right are good electron acceptors. They oxidize other species by accepting electrons. The (ω-) values of the studied cations are larger than those of their complexes, on the contrary, the (ω+) values of the studied cations are smaller than those of their complexes. Fig. 5 shows that Be cation is the best electron acceptor and adsorption energy of its complexes for Be-Is_a is the highest (-295.81kcal/mol).

3. Conclusion

Be-Is_a, Mg-Is_a, Ca-Is_a, Be-Is_b, Mg-Is_b, Ca-Is_b complexes were calculated theoretically in gas phase using DFTB3LYP/6-311G (d, p) method. HOMA values of the Be-Is_a, Mg-Is_a, Ca-Is_a, Be-Is_b, Mg-Is_b, Ca-Is_b complexes is less than that of free Is. The adsorption energy, enthalpy and Gibbs free energy of the Be-Is_a, Mg-Is_a, Ca-Is_a, Be-Is_b, Mg-Is_b, Ca-Is_b complexes decrease with the increase of ion size (Be^{2+}, $Mg^{2+}$and Ca^{2+}). The negative value of E_{HOMO}, and E_{LUMO} of the complexes decrease according to free Is. The strongest bond was calculated for Be-Is_a complex according to QTAIM result. It can be defined partially covalent character. However, the weak interactions of Is molecule with Mg and Ca cations are non-covalent type. This is also evidenced by the colour filled RDG isosurfaces created with VMD for Is-Be^{2+} and Is-Mg^{2+} complexes. According to DAM, Mg-Is_b complex is the worst electron donor and the best electron acceptor.

References

[1] J. Bergman, J-O Lindström, U. Tilstam, The structure and properties of some indolic constituents in Couroupita guianensis aubl, Tetrahedron. 41(14) (**1985**) 2879-2881. https://doi.org/10.1016/S0040-4020(01)96609-8

[2] M. Yoshikawa, T. Murakami, A. Kishi, T. Sakurama, H. Matsuda, M. Nomura, H. Matsuda, M. Kubo, Novel indole S, O-bisdesmoside, calanthoside, the precursor glycoside of tryptanthrin, indirubin, and isatin, with increasing skin blood flow promoting effects, from two Calanthe species (Orchidaceae), Chem. Pharm. Bull, 46(5) (**1998**) 886-888. https://doi.org/10.1248/cpb.46.886

[3] M. d'Ischia, A. Palumbo, G. Prota, Adrenalin oxidation revisited. New products beyond the adrenochrome stage, Tetrahedron. 44(20) (**1988**) 6441-6446. https://doi.org/10.1016/S0040-4020(01)89832-X

[4] A. Palumbo, M. d'Ischia, G. Misuraca, G. Prota, A new look at the rearrangement of adrenochrome under biomimetic conditions, Biochim. Biophys. Acta. 990(3) (**1989**) 297-302. https://doi.org/10.1016/S0304-4165(89)80048-0

[5] J. Halket, P.J. Watkins, A. Przyborowska, B.L. Goodwin, A. Clow, V. Glover, M. Sandler, Isatin (indole-2,3-dione) in urine and tissues: detection and determination by gas chromatography—mass spectrometry, Journal of Chromatography B: Biomedical Sciences and Applications. 562 (1-2) (**1991**) 279-287. https://doi.org/10.1016/0378-4347(91)80585-Z

[6] A. Boukaoud, Y. Chiba, D. Sebbar, M. Dehbaoui, N. Guechi, A Theoretical Study of Vibrational and Optical Properties of Isatin, Braz. J Phys. 51 (**2021**) 1207–1214. https://doi.org/10.1007/s13538-021-00924-5

[7] P. Naumov, F. Anastasova, Experimental and theoretical vibrational study of isatin, its 5-(NO2, F, Cl, Br, I, CH3) analogues and the isatinato anion, Spectrochimica Acta Part A: Molecular and Biomolecular Spectroscopy. 57(3) (**2001**) 469-481. https://doi.org/10.1016/S1386-1425(00)00393-0

[8] L. Kilian, A. Hausschild, R. Temirov, S. Soubatch, A. Schöll, A. Bendounan, F. Reinert, T.L. Lee, F.S. Tautz, M. Sokolowski, E. Umbach, Role of Intermolecular Interactions on the Electronic and Geometric Structure of a Large π-Conjugated Molecule Adsorbed on a Metal Surface, Phys. Rev. Lett. 100 (**2008**). 136103. https://doi.org/10.1103/physrevlett.100.136103

[9] B. Fiedler, W. Reckien, T. Bredow, J. Beck, M. Sokolowski, Structure and Charge Transfer in Binary Ordered Monolayers of Two Sulfur-Containing Donor Molecules and TNAP on the Au(111) Surface,. J. Phys. Chem. C. 118 (**2014**) 3035–3048. https://doi.org/10.1021/jp407579z

[10] S.D.A. Kumar, R.T Koyadeen, A Methedology to Simulate and Analyse Molecules as Molecular Switches. Int. J. Simul.-Syst. Sci. Technol. 17 (**2016**) 22. https://doi.org/10.5013/IJSSST.a.17.32.22

[11] T.R., Koydeen, D.A., Kumar, R. Raj, Simulation and Analysis of BDT Molecule with Au Electrodes as a Molecular Switch UKSim-AMSS 18th International Conference on Computer Modelling and Simulation (UKSim). IEEE, 2016. Page(s):87 – 92

[12] K.K. Bania, A. K. Guha, P.K. Bhattacharyya, S. Sinha, Effect of substituent and solvent on cation–π interactions in benzene and borazine: a computational study, Dalton Trans 43(176) (**2014**) 1769–1784. https://doi.org/10.1039/C3DT52081A

[13] F. Genc, F. Kandemirli, S. Senturk Dalgic, A theoretical study on 1H-indole-2,3-dione complexes with lithium, sodium, and potassium cation, J Mol Model 30(4), (**2024**) 100. https://doi.org/10.1007/s00894-024-05898-0

[14] T. Lu, F. Chen, MULTIWFN: a multifunctional wave function analyser, J. Comput. Chem. 33 (2012) 580–592. https://doi.org/10.1002/jcc.22885

[15] W. Humphrey, A. Dalke.; K. Schulten, VMD: Visual Molecular Dynamics. J. Mol. Graphics 14 (1996). 33−38. https://doi.org/10.1016/0263-7855(96)00018-5

[16] M.J. Frisch, G.W. Trucks, H.B, Schlegel G.E., Scuseria, M.A., Robb, J.R. Cheeseman, G. Scalmani, V. Barone, et al., (**2013**) Gaussian 09. Gaussian Inc., Wallingford. https://doi.org/10.1017/CBO9781107415324.004

[17] A.D. Becke, Density-functional thermochemistry. III. The role of exact Exchange J. Chem. Phys 98 (**1993**) 648-5652. https://doi.org/10.1063/1.464913

[18] C. Lee, W. Yang, R.G Parr, Development of the Colle-Salvetti correlation-energy formula into a functional of the electron density, Phys Rev B Condens Matter. 15;37(2), (**1998**). 785-789. https://doi.org/10.1103/PhysRevB.37.785

[19] S.F, Boys, R. Bernardi, The calculation of small molecular interactions by the differences of separate total energies. Some procedures with reduced errors, Mol. Phys. 19 (**1970**). 553-566. https://doi.org/10.1080/00268977000101561

[20] H.R. Ghenaatian, Structural and electronic properties of alumaphosphinine complexes with metal ions: A theoretical study, Sharif University of Technology Scientia Iranica Transactions C: Chemistry and Chemical Engineering 24(3) (**2017**) 1181-1188. doi:10.24200/SCI.2017.4099

[21] R.F.W Bader, A bond path: A universal indicator of bonded interactions", J. Phys. Chem. A 102 (**1998**) 7314-7323. https://doi.org/10.1021/jp981794v

[22] R., Parthasarathi, V. Subramanian, N. Sathyamurthy Hydrogen bonding without borders: an atoms-in-molecules perspective, J Phys Chem A 16;110(10) (**2006**) 3349-3351. https://doi.org/10.1021/jp060571z

[23] Y. Hirano, K. Takeda, K. Miki, Charge-density analysis of an iron–sulfur protein at an ultra-high resolution of 0.48 Å, Nature 534 (**2016**) 281-284. https://doi.org/10.1038/nature18001

[24] H. S. Sayiner, F. Kandemirli, S. Senturk Dalgic, M. Monajjemi, F. Mollaamin. Carbazochrome carbon nanotube as drug delivery nanocarrier for anti-bleeding drug: Quantum chemical study. J Mol Model. 28(1) (2022) 11. https://doi.org/10.1007/s00894-021-04948-1

[25] Z. H. Al-Sawaff, S. Senturk Dalgic, F. Kandemirli, A Density Functional Theory (DFT) Study on Silicon Doped Carbon Nanotube Si-CNT as a Carrier for BMSF-BENZ Drug used for Osteoporosis Disease, Momento 65 (2022) 1-24. https://doi.org/10.15446/mo.n65.99010

[26] M. D. Mohammadi, H. Y. Abdullah, Intermolecular Interactions between Serine and C_{60}, $C_{59}Si$, $C_{59}Ge$: a DFT Study. Silicon 14 (2022) 6075-6088. https://doi.org/10.1007/s12633-021-01408-6

[27] S. Senturk Dalgic, F. Kandemirli, DFT based calculations of Acid Molecules on 2D C3N nanosheets:

QTAIM, NCI Analysis. J. mater. Electron. Device 5 (2021) 1-6.
[28] C. Matta, R.J. Boyd The Quantum Theory of Atoms in Molecules: From Solid State to DNA and Drug Design Chapter 1. An Introduction to the Quantum Theory of Atoms in Molecules. https://doi.org/10.1002/9783527610709.ch1
[29] D. Cremer, E. Kraka Chemical bonds without bonding electron density – does the difference electron-density analysis suffice for a description of the chemical bond? Angew. Chem. Int. Ed. Engl. 23 (**1984**) 627–628. https://doi.org/10.1002/anie.198406271
[30] J.A. Pople, J.S. Binkley, R. Seeger, Theoretical models incorporating electron correlation. Int. J. Quantum Chem., Symp., 10 (**1976**) 1-19. https://doi.org/10.1002/qua.560100802
[31] M. Ziolkowski, S.J. Grabowski, J, Leszczynski, Cooperativity in hydrogen-bonded interactions: ab initio and atoms in molecules analyses, J. Phys. Chem. A, 110, (**2006**) 514-6521. https://doi.org/10.1021/jp060537k
[32] E.R. Johnson, S. Keinan, P. Mori-Sánchez, J. Contreras-García, A.J. Cohen, W. Yang, Revealing noncovalent interactions, J Am Chem Soc. 132(18) (**2010**) 6498–6506. https://doi.org/10.1021/ja100936w
[33] S. Dalgic Senturk, Z.H. Al-Sawaff, S. Dalgic, F. Kandemirli, A comparative DFT study on Al- and Si- doped single wall carbon nanotubes (SWCNTs) for Ribavirin drug sensing and detection, Material Science in Semiconductor Process. 158 (**2023**). 107360. https://doi.org/10.1016/j.mssp.2023.107360
[34] T.M Krygowski, Crystallographic studies of intermolecular and intramolecular interactions reflected in aromatic character of p-electron systems, The Journal for Chemical Information and Computer Sciences. 33 (**1993**) 70–78. https://doi.org/10.1021/ci00011a011
[35] T.M. Krygowski, M. Cyranski, Separation of the energetic and geometric contributions to the aromaticity of p-electron carbocyclics, Tetrahedron. 52 (**1996**) 1713–1722. https://doi.org/10.1016/0040-4020(95)01007-6
[36] J. Kruszewski, T.M.Krygowski, Definition of aromaticity basing on harmonic oscillator model. Tetrahedron Letters. 13 (**1972**) 3839–3842. https://doi.org/10.1016/S0040-4039(01)94175-9
[37] C.W. Bird, A new aromaticity index and its application to five-membered ring heterocycles, Tetrahedron. 41(7) (**1985**) 1409-1414. https://doi.org/10.1016/S0040-4020(01)96543-3